# On the Greenhouse Effect

Claude Bardos, Olivier Pironneau

# On the Greenhouse Effect

Claude Bardos[*]  & Olivier Pironneau[†]

January 13, 2021

### Abstract

Radiative transfer is at the heart of the mechanism to explain the greenhouse effect due to carbon dioxide, methane and others in the earth atmosphere. We revisit this much studied field from a mathematical and numerical point of view. Existence and uniqueness and semi-analytic solutions of the Milne problem for grey atmospheres are stated. Numerical simulations are given for grey and non grey atmosphere and applied to the greenhouse effect. It is found that greenhouse gases are indeed capable of making the earth temperature 1 or $2^o$C hotter, even without taking into account the complexity of a full ocean-atmosphere-biosphere climate model.

## 1 Introduction

The greenhouse effect is an important element of the current theory of climate change. Some gases in the earth atmosphere like carbon dioxide $CO_2$ and methane $CH_4$ absorb infrared rays and thus contribute to a global warming of our planet. As explained in [1], [17] and [9] the sun radiates light with a heat flux $Q_0 = 1370$Watt/m$^2$, in the frequency range $(0.5, 20)10^{14}$ corresponding approximately to a black body at temperature of 5800K; 70-75% of this light intensity reaches the ground because the atmosphere is almost transparent to this spectrum but about 30% is reflected by the clouds or the ground (albedo).

The earth behaves almost like a black body at temperature $T_e = 288K$ and as such radiates rays of frequencies $\nu$ in the infrared spectrum $(0.03, 0.6)10^{14}$.

So both the sun and the earth are approximate black bodies. The Planck theory says that a black body at temperature $T$ radiates electromagnetic waves in the entire frequency spectrum $\nu \in \mathbb{R}^+$ with intensities given by the Planck function:

$$\nu \in \mathbb{R}^+ \mapsto B_\nu(T) = \frac{2\hbar\nu^3}{c^2[e^{\frac{\hbar\nu}{kT}} - 1]} \tag{1}$$

where $\hbar$ is the Planck constant, $c$ is the speed of light and $k$ is the Boltzmann constant.

A major discrepancy between reality and the black body theory for earth is shown on fig 2. It is due to the absorption power of $CO_2$, $H_2O$, $O_3$, $CH_4$, etc, in the infrared range. Figure 1 gives the transmission coefficients $\kappa_n u$ for some gas (a tranparent gas has $\kappa_\nu = 1$ ,and zero if it is opaque.) Consequently the infrared light emitted by earth, seen from far, has a defect of energy in its spectrum; the energy defect is changed to heat: it is the *greenhouse effect*.

In this article we propose a mathematical and numerical investigation to quantify this phenomenon.

Photons travel at the speed of light; energy balance can thus be assumed instantaneous. The atmosphere is affected by wind, rain, chemistry, etc, but at a very different time-scale; it is believed – and to some extent demonstrated, (see [9]) – that even if all these other phenomena are ignored, still the greenhouse effect is sufficient to explain partially global warming. Consequently, in the article, we restrict the analysis to the energy conservation equations for the radiative intensity and the temperature, equations (3) and (4) below.

---

[*]*claude.bardos@gmail.fr*, LJLL, Université de Paris, France.

[†]*olivier.pironneau@sorbonne-universite.fr*, LJLL, Sorbonne Université, Paris, France.
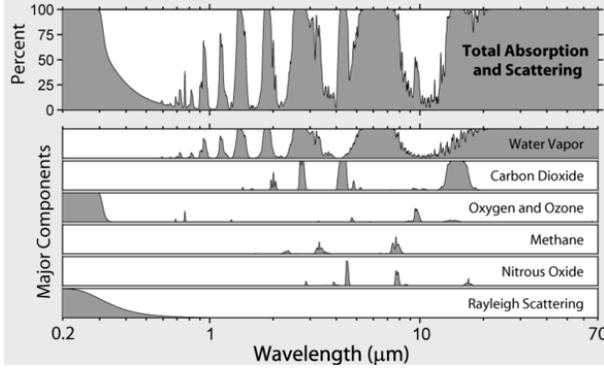
Figure 1: *Absorption coefficient $\kappa_\nu$ of several gases of the earth atmosphere show in the range of frequencies of interest, but versus wave length (speed of light $/\nu$). (reprinted from wikipedia).*
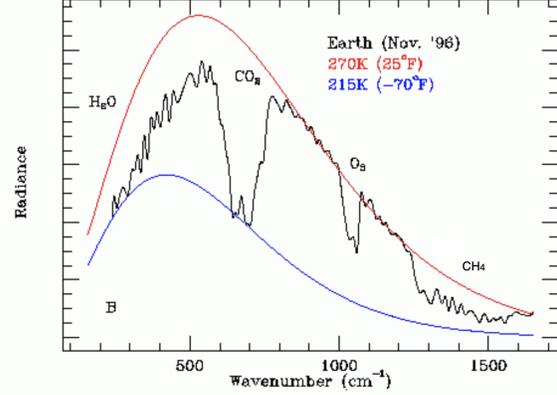


Figure 2: *The thermal infrared emission spectrum of the Sahara, as recorded from deep space by the Mars Global Surveyor (MGS) Spacecraft in November 1996, (reprinted from xylenepower.com.)*

Radiative transfers have been studied by astronomers and nuclear physicists. Their work are summarized in [12] and [14]. Mathematical analysis are also numerous and we send the readers to [8], [10] and [25].

More recently, for obvious reasons, there is a regain of interest in numerical simulations of radiative transfers. Among others the reader is sent to [21],[18], [19],[20], [23]. However we are not aware of a simulation of the very specific greenhouse gases (GHG) effect, as presented here.

## 2 The fundamental equations

Let $I_\nu(\mathbf{x}, \omega)$ be the intensity of the radiation of frequency $\nu$ in the direction $\omega$ at point $\mathbf{x}$ of the physical domain $\Omega$. The average operator on the unit sphere $\mathbb{S}^2$ is denoted by $\oint$ ; for instance,

$$\oint I_\nu(\omega)\mathrm{d}\omega := \frac{1}{4\pi} \int_{\mathbb{S}^2} I_\nu(\omega)\mathrm{d}\omega. \tag{2}$$

Let $T(\mathbf{x})$ be the temperature . Energy balance (see [14],[9]) yields,

$$\omega \cdot \nabla I_\nu + \rho \kappa_\nu a_\nu \left[ I_\nu - \oint p(\omega, \omega') I_\nu(\omega')\mathrm{d}\omega' \right] = \rho \kappa_\nu (1 - a_\nu)[B_\nu(T) - I_\nu], \tag{3}$$

$$-\kappa_T \Delta T = \nabla \cdot \int_0^\infty \oint I_\nu(\omega')\omega' \mathrm{d}\omega' \mathrm{d}\nu. \tag{4}$$

Here, $\rho(\mathbf{x})$ is the density of the medium, $\kappa_\nu$ is the absorption coefficient (percentage absorbed per unit length), $a_\nu$ is the scattering coefficient; $p(\omega, \omega')$ is the probability that a ray in the direction $\omega'$ scatter in the direction $\omega$; both $\kappa_\nu$ and $a_\nu$ usually depend on $\nu$, and even $\mathbf{x}$. The constant $\kappa_T$ is the thermal diffusion.

As usual, boundary conditions have to be given. For the temperature we may prescribe its normal derivative to be zero for all $\mathbf{x} \in \partial\Omega$. The equation for the intensity being a first order "kinetic" equation, $I_\nu$ must be given where particles penetrate the domain $\Omega$. Therefore with $\mathbf{n}(\mathbf{x})$ being the outward normal to the boundary $\partial\Omega$ one denotes by

$$\Sigma_+ = \{(\mathbf{x}, \omega) \in \partial\Omega \times \mathbb{S}^2\} \quad \text{with} \quad \mathbf{n}(\mathbf{x}) \cdot \omega > 0, \quad \Sigma_- = \{(\mathbf{x}, \omega) \in \partial\Omega \times \mathbb{S}^2\} \quad \text{with} \quad \mathbf{n}(\mathbf{x}) \cdot \omega < 0. \tag{5}$$

In most case no boundary condition is given on $\Sigma_+$ while a boundary condition is prescribed on $\Sigma_-$ i.e. on the incoming flux of particles. Alternatively one can also (see below) use on $\Sigma_-$ some of the information arriving on $\Sigma_+$ .

2

## 2.1 Isotropic scattering

When $p(\omega, \omega') \equiv 1$, the equations can be simplified due to the following

**Proposition 1**

$$\nabla \cdot \int_{\mathbb{S}^2} I_\nu(\omega)\omega\, d\omega = \rho\kappa_\nu(1 - a_\nu)\left(4\pi B_\nu(T) - \int_{\mathbb{S}^2} I_\nu(\omega)\, d\omega\right). \tag{6}$$

*Proof.* It is shown by averaging (3) on $\mathbb{S}^2$ as in (2).

**Corollary 1** *The temperature equation which is normally written with a flux of radiative energy (4), can also be recast as (7):*

$$-\kappa_T \Delta T - \int_0^\infty \rho\kappa_\nu(1 - a_\nu)\left(B_\nu(T) - \oint I_\nu(\omega)d\omega\right) d\nu = 0. \tag{7}$$

**Corollary 2** *If the thermal diffusion $\kappa_T$ is neglected in (7), then*

$$\int_0^\infty \kappa_\nu(1 - a_\nu)B_\nu\, d\nu = \int_0^\infty \kappa_\nu(1 - a_\nu) \oint I_\nu(\omega)\, d\omega\, d\nu. \tag{8}$$

**Remark 1** *When $\kappa_\nu$ and $a_\nu$ are constant, (8) leads to the Stefan-Blotzmann law*

$$\sigma_b T^4 = \int_0^\infty \oint I_\nu(\omega)d\omega\, d\nu, \ \ with \ \sigma_b = \frac{2\hbar}{15c^2}\left(\frac{k\pi}{\hbar}\right)^4. \tag{9}$$

Some proofs concerning the existence, uniqueness and stability for solutions of simplified versions of this problem appear below. The most general case is discussed in the conclusion with relevant and updated references.

# 3   One dimensional Approximations

**Proposition 2** *Consider (3),(7) in a vertical slab $\Omega = (0, H) \times \mathbb{R}^2$. Assume that the boundary conditions at $\mathbf{x} = (x, y, z)$ are independent of $y, z$, and assume isotropic scattering ($p \equiv 1$). Then, the solution depends only on $x$ and $\mu = \cos\phi = \omega \cdot \mathbf{n}$; $I_\nu(\mathbf{x}, \omega) = I'_\nu(x, \mu)$ is given by: for all $x \in (0, H)$, $\mu \in (-1, 1)$,*

$$\mu\partial_x I'_\nu + \rho\kappa_\nu a_\nu\left(I'_\nu - \frac{1}{2}\int_{-1}^1 I'_\nu(x, \mu)d\mu\right) + \rho\kappa_\nu(1 - a_\nu)[I'_\nu - B_\nu] = 0, \tag{10}$$

*Proof.* : Both problems (3),(7)) and (10) have one and only one solution. Let us show that $I_\nu(x, y, \omega_1, \omega_2) = I'_\nu(x, \cos\phi)$ is a solution of (3),(7)) when $I'_\nu$ is a solution of (10).

Let $t$ be the direction of the projection of $\omega$ on the plan $P$ of the slab boundary. $I_\nu$ is invariant in $t$. Hence with $\omega = \{\omega_1, \omega_2\} = \{cos\phi, \sin\phi\}^T$,

$$\omega\nabla I_\nu = \omega_1\partial_x I_\nu + \omega_2\partial_t I_\nu = \cos\phi\partial_x I'_\nu + \sin\phi\partial_t I'_\nu = \cos\phi\partial_x I'_\nu + 0 = \mu\partial_x I'_\nu.$$
$$\frac{1}{4\pi}\int_{\mathbb{S}^2} I_\nu(x, \mu)d\omega = \frac{1}{4\pi}\int_0^{2\pi}\int_{-\pi}^\pi I'_\nu(x, \cos\phi)(-\sin\phi)d\phi d\psi = \frac{1}{2}\int_{-1}^1 I'_\nu(x, \mu)d\mu.$$

$\square$

**Corollary 3** *If light hits the right vertical boundary at a constant angle $\theta$ and intensity $Q_\nu = Q_0\tilde{Q}_\nu$ and there is total light absorption on the upper half right boundary, i.e.*

$$I'_\nu(H, \mu) = 0, \forall\mu \in (-1, 0), \quad I'_\nu(0, \mu) = \mu Q_\nu\cos\theta, \forall\mu \in (0, 1), \tag{11}$$

*then $I'$ is uniquely defined by (10)(11) and it is proportional to $Q_0\cos\theta$.*

**Remark 2** *Boundary conditions (11) will be used throughout below.* **It is important to understand their implications**. *First it assumes that an horizontal beam of energy $Q_0$ hitting a plan with an the angle $\theta$ with the normal, is the same as a vertical beam of intensity $Q_0 \cos \theta$.*

Hence to compute $T$ at all points of planet earth, one needs only to compute it at the point of intersection of the sphere and the sun-earth line and then multiply by $\cos \theta$. Reality is definitely more complex because this theory implies that the earth temperature at night is zero Kelvin!

In (11) the sun is on the right of planet earth and sunlight crosses the earth atmosphere without interaction till it hits the ground. The intensity of light emitted by the ground at an angle $\phi$ is proportional to $Q_0 \cos \theta$, and to $\cos \phi$.

Finally condition (11) implies that nothing returns to space on the dark side of the light direction $\phi$, i.e. $\phi > \frac{\pi}{2}$.

**Note** . *We focus on the interaction between temperature and light intensity; hence for clarity we neglect the scattering, i.e. $a_\nu = 0$. Note however that much of what is derived below apply also in case of isotropic scattering.*

## 3.1 Spherical symmetry

Consider a spherical planet receiving light rays from a direction $\mathbf{i}$. The planet's radius is $R$ and its atmosphere is $\Omega = \{\mathbf{x} \in \mathbb{R}^3, |R| < |\mathbf{x}| < R + H\}$ . Let us use spherical coordinates: $r = |\mathbf{x}| - R$ , $\psi$ the azimuthal angle with respect to an axis parallel to the rays $\mathbf{i}$, and $\theta$ the latitude angle. Invariance with respect to $\psi$ and a similar argument as above (see [12]) leads to the Chandrasekhar correction:

$$\mu \frac{\partial \bar{I}_\nu}{\partial r} + \frac{1 - \mu^2}{R + r} \frac{\partial \bar{I}_\nu}{\partial \mu} + \kappa_\nu \rho \left( \bar{I}_\nu - B_\nu(T) \right) = 0, \quad \forall r, \mu, \nu \in (0, H) \times (-1, 1) \times \mathbb{R}^+. \tag{12}$$

and if thermal diffusion is neglected:

$$\int_0^\infty \rho \kappa_\nu \left( B_\nu(T) - \frac{1}{2} \int_{-1}^1 \bar{I}_\nu d\mu \right) d\nu = 0, \quad \forall r \in (0, H). \tag{13}$$

Note that no additional boundary condition to (11) is needed because $1 - \mu^2$ is zero at $\mu = \pm 1$.

These "Chandrasekhar equations" can be adimensionalised by introducing a length scale $\lambda$, scaling factors for $B$, $\nu$ and $\rho$ and set: $r = \tilde{r}\lambda$, $R = \tilde{R}\lambda$ and $H = \tilde{H}\lambda$, $\rho = \rho_0 \tilde{\rho}$ and $B = B_0 \tilde{B}$. Then we may rewrite the above and its boundary conditions as :

$$\mu \frac{\partial \tilde{I}_\nu}{\partial \tilde{r}} + \frac{1 - \mu^2}{\tilde{R} + \tilde{r}} \frac{\partial \tilde{I}_\nu}{\partial \mu} + \tilde{\kappa}_\nu \tilde{\rho} \left( \tilde{I}_\nu - \tilde{B}_\nu(\tilde{T}) \right) = 0, \quad \int_0^\infty \tilde{\kappa}_\nu \left( \tilde{B}_\nu(\tilde{T}) - \frac{1}{2} \int_{-1}^1 \tilde{I}_\nu d\mu \right) d\tilde{\nu} = 0,$$
$$\tilde{I}_\nu(H, \mu) = 0, \forall \mu \in (-1, 0), \quad \tilde{I}_\nu(0, \mu) = \mu B_0^{-1} Q_\nu \cos \theta, \forall \mu \in (0, 1) \tag{14}$$

with

$$\tilde{\kappa}_\nu = \lambda \rho_0 \kappa_\nu, \quad \tilde{B} = B_0^{-1} \frac{2h\nu_0^3}{c^2} \frac{\tilde{\nu}^3}{e^{\frac{\tilde{\nu}}{\tilde{T}}} - 1}, \quad T = \frac{\hbar \nu_0}{k} \tilde{T}, \quad \bar{I}_\nu = B_0 \tilde{I}_\nu. \tag{15}$$

## 3.2 Evanescent atmosphere

When $\rho = \rho_0 e^{-\tilde{r}}$, we make a last change of variable (analogous to the optical depth introduced in physics) to cope with that exponentially rarefying atmosphere: $(r, \mu) \to (\tau := 1 - e^{-\tilde{r}}, \mu)$. Then, with $Z = 1 - e^{-\tilde{H}}$, for all $\tau, \mu, \nu \in (0, Z) \times (-1, 1) \times \mathbb{R}^+$,

$$\mu \frac{\partial \tilde{I}_\nu}{\partial \tau} + \gamma(\tau, \mu) \frac{\partial \tilde{I}_\nu}{\partial \mu} + \tilde{\kappa}_\nu \left( \tilde{I}_\nu - \tilde{B}_\nu \right) = 0, \quad \int_0^\infty \tilde{\kappa}_\nu \left( \tilde{B}_\nu(T) - \frac{1}{2} \int_{-1}^1 \bar{I}_\nu d\mu \right) d\tilde{\nu} = 0.$$

$$\tilde{I}_\nu(Z,\mu) = 0, \forall \mu \in (-1,0), \quad \tilde{I}_\nu(0,\mu) = \mu\tilde{Q}_\nu, \forall \mu \in (0,1), \tag{16}$$

where $\tilde{Q}_\nu = Q_\nu \cos\theta/B_0$. The Chandrasekhar correction is

$$\gamma(\tau,\mu) = \frac{1-\mu^2}{(1-\tau)(\tilde{R} - \log(1-\tau))} \tag{17}$$

**Remark 3** *For clarity, from now on, we drop the tildes.*

## 3.3   Grey atmosphere

By definition, in a grey atmosphere (Fowler [9] p70), nothing depends on $\nu$. If in addition the thermal diffusion is neglected, i.e. $\kappa_T = 0$, then the total radiation intensity, $I = \int_0^\infty I_\nu d\nu$, is given by (11) and

$$\mu\partial_x I + \gamma\partial_\mu I = \rho\kappa[B - I] \text{ with } B = \int_0^\infty B_\nu(T)d\nu = \frac{1}{2}\int_{-1}^1 I d\mu. \tag{18}$$

Temperature is recovered from $B = \sigma_b T^4$.

## 3.4   The multi-groups problem

In numerical computations one replace the continuous dependance of the frequency $I_\nu$ by a finite set of frequencies $I_k$ and this is also the case for climate modelling.

Hence one introduces $I_k$ the intensity of photons with frequency $\nu_k$ and write the system: for $k = 1..N$,

$$\mu\frac{\partial I_k}{\partial \tau} + \gamma(\tau,\mu)\frac{\partial I_k}{\partial \mu} + \kappa_{\nu_k}(I_k - B_{\nu_k}(T)) = 0, \quad \sum_k \kappa_{\nu_k}\left(B_{\nu_k}(T) - \frac{1}{2}\int_{-1}^1 \bar{I}_k d\mu\right)d\nu = 0.$$
$$I_k(Z,\mu) = 0, \forall \mu \in (-1,0), \quad I_k(0,\mu) = \mu Q_{\nu_k}, \forall \mu \in (0,1). \tag{19}$$

Recall that $T$, which is a function of $\tau$ only, couples all the $I_k$.

This formulation will be used in the numerical section 7.

## 3.5   The Milne problem

When $\gamma$ is neglected in (18), the problem is known as Milne's problem in $\Omega = (0,Z) \times (-1,1)$:

$$\mu\frac{\partial I}{\partial \tau} + \kappa\left(I - \frac{1}{2}\int_{-1}^1 I d\mu\right) = 0, \ \forall \tau, \mu \in \Omega, \quad I(Z,\mu) = g_H, \ \forall \mu \in (-1,0), \quad I(0,\mu) = \mu, \ \forall \mu \in (0,1). \tag{20}$$

where $\kappa = \kappa_\nu \rho$ is constant.

# 4   More about the Milne problem

Emphasis on the Milne problem is motivated by the two following facts.

- It correspond to a local in space description of the atmosphere say of eight $H$ because for $R$ large compared to $H$ the Chandrasekhar correction can be neglected.

- One can introduce the point of view of functional analysis (cf. [8] chapter 21 Vol 9) without going into details but keeping things *as explicit as possible.*

- One can also use very explicit computations which were derived at the time when computers were not available, say in the middle of the previous century .

We consider the abstract problem (22).

**Theorem 1** *With*

$$f(x,\mu) \in L^2((0,H) \times (-1,1)) \quad \mu^{\frac{1}{2}} g_0(\mu) \in L^2(0,1) \quad and \quad |\mu|^{\frac{1}{2}} g_H(\mu) \in L^2(-1,0) \tag{21}$$

*the problem*

$$\mu \partial_x I + I - \frac{1}{2} \int_{-1}^{1} I(x,\mu') d\mu' = f, \ I(0,\mu)|_{\mu>0} = g_0(\mu), \ I(H,\mu)|_{\mu<0} = g_H(\mu), \tag{22}$$

*has a unique solution* $I \in L^2((0,H) \times (-1,1)))$ *which satisfies the estimates:*

$$\|I\|_{L^2((0,H) \times (-1,1))} \leq C(H)\{\|I\|_{L^2((0,H) \times (-1,1))} + \|\mu^{\frac{1}{2}} g_0(\mu)\|_{L^2(0,1))} + \||\mu|^{\frac{1}{2}} g_H(\mu)\|_{L^2(-1,0))} \tag{23a}$$

*Moreover when the data* $f, g_0, g_H$ *are non negative , the same is true for* $I$*, the solution of (22). With* $f = 0$
*one has:*

$$\sup I(x,\mu) \leq \sup \Big( \sup_{\mu \in (0,1)} g_0(\mu), \sup_{\mu \in (-1,0)} g_H(\mu)) \Big). \tag{23b}$$

*Proof.* The leading ideas are given below while details can be found in ([8]) . They are all based on the estimate of physical quantities which are translated into "mathematical" norms. When unambiguous, the symbol $\|.\|$ will be used below to denote, any $L^2$ norm in $(L^2((0,H) \times (-1,1))$ , $L^2_\mu(-1,1)$, $L^2_\mu(0,1))$ and $L^2_\mu(-1,0))$ . Observe that the formula

$$I(x,\mu) = \frac{1}{2} \int I(x,\mu) d\mu + (I(x,\mu) - \frac{1}{2} \int I(x,\mu) d\mu) \tag{24}$$

gives the decomposition of $I \in L^2_\mu(-1,1)$ in its orthogonal projection on the space of independent of $\mu$ functions and on its orthogonal (i.e. function of 0 $\mu$ average) . Hence one introduces for $\epsilon \geq 0$ the regularized equation:

$$\epsilon I_\epsilon + \mu \partial_x I_\epsilon + I_\epsilon - \frac{1}{2} \int_{-1}^{1} I_\epsilon(x;\mu') d\mu' = f(x,\mu) , \ I(0,\mu)|_{\mu>0} = g_0(\mu), \ I(H,\mu)|_{\mu<0} = g_H(\mu). \tag{25}$$

**A priori estimate and uniqueness**

Multiplying this equation by $I_\epsilon$, integrating with respect to $x$ the term leads to,

$$(\partial_x I_\epsilon)(I_\epsilon) = \frac{1}{2} \partial_x I_\epsilon^2;$$

taking in account the fact that $I$ coincides on $\Sigma_-$ with the incoming data $g_0$ or $g_H$ using the Cauchy Schwartz formula one obtains:

$$\epsilon \|I_\epsilon\|^2_{L^2((0,H)(-1,1))} + \|I_\epsilon - \frac{1}{2} \int_{-1}^{1} I_\epsilon(x,\mu') d\mu'\|^2_{L^2((0,H)(-1,1))}$$
$$\leq \|I_\epsilon\|_{L^2((0,H)(-1,1))} \|f\|_{L^2((0,H)(-1,1))} + \||\mu|^{\frac{1}{2}} I_\epsilon\|_{L^2(\Sigma_-)} \||\mu|^{\frac{1}{2}} g(x,\mu)\|_{L^2(\Sigma_-)} . \tag{26}$$

Since the problem is linear, denoting by $\tilde{I}$ the difference of two solutions with the same boundary data $g_0$ and $g_H$ and same external density $f$ , one deduces from (26) the uniqueness (for $\epsilon > 0$) of the solution of the problem (22) according to the estimate:

$$\epsilon \|\tilde{I}_\epsilon\|^2_{L^2((0,H) \times (-1,1))} + \|\tilde{I}_\epsilon - \frac{1}{2} \int_{-1}^{1} \tilde{I}_\epsilon(x,\mu') d\mu'\|^2_{L^2((0,H) \times (-1,1))} \leq 0 \tag{27}$$

To extend this observation to the case $\epsilon = 0$ one observes that in such case (27) gives:

$$\|\tilde{I}_\epsilon - \frac{1}{2} \int_{-1}^1 \tilde{I}_\epsilon(x,\mu')d\mu'\|^2_{L^2((0,H)(-1,1))} = 0 \tag{28}$$

which gives the relation

$$\mu \partial_x \tilde{I} = 0, \text{ with } \tilde{I}(0,\mu) = 0 \text{ for } \mu > 0, \text{ and with } \tilde{I}(H,\mu) = 0 \text{ for } \mu < 0 \tag{29}$$

which implies $\tilde{I} = 0$.

$\diamond$

**Existence of Solutions for $\epsilon > 0$**
    For clarity the proof of the estimate (26) and of the existence of a solution are done in the absence of boundary source. Then, using the linearity of the problem it can be easily adapted to more general situations. First with $\epsilon > 0$ for (26) one obtains a trivial stability estimate

$$\|\tilde{I}_\epsilon\|^2_{L^2((0,H)\times(-1,1))} \leq \frac{1}{\epsilon}\|f\|^2_{L^2((0,H)\times(-1,1))} \tag{30}$$

    To prove the existence of the solution one consider with $\epsilon > 0$ the Milne problem (22) in an iterative form first with $g_0 = g_H = 0$.

$$(1+\epsilon)I_\epsilon^{n+1} + \mu\partial_x I_\epsilon^{n+1} = \frac{1}{2}\int_{-1}^1 I_\epsilon^n(x;\mu')d\mu' + f(x,\mu) \tag{31}$$

leading to the estimate

$$\|I_\epsilon^{n+1}\| \leq \frac{1}{1+\epsilon}(\|I_\epsilon^n\| + \|f\|) \tag{32}$$

which shows that the mapping $I_\epsilon^n \mapsto I_\epsilon^{n+1}$ is a strict contraction.
    Then the same type of proof works also for the case $f = 0$ with non zero incoming data on $\Sigma_-$ with the estimate:

$$\|I_\epsilon^{n+1}\|^2 \leq \frac{1}{1+\epsilon}(\|I_\epsilon^n\|^2 + \int_0^1 \mu|g_0(\mu)| + \int_{-1}^0 |\mu|g_H(\mu)|^2) \tag{33}$$

and the solution of the general problem with $\epsilon > 0$ non zero $f$ and non zero ($g_0$ and $g_H$) follows by linearity. The above construction will be used to prove convergence of the numerical method in the second part of the paper.

**Existence of a solution for $\epsilon = 0$**
    To let $\epsilon \to 0$, one proceeds with the following contradiction argument. If there would be no finite constant $C$ for which holds the relation:

$$\|\tilde{I}_\epsilon\|^2_{L^2((0,H)\times(-1,1))} \leq C\|f\|^2_{L^2((0,H)\times(-1,1))} \tag{34}$$

that would imply the existence of a family of functions $f_\epsilon$ of $L^2((0,H)\times(-1,1))$ with norm equal to 1 while the corresponding solution of $I_\epsilon$ would go to infinity in the same norm . Then it generates a solution to the problem:

$$\tilde{f}_\epsilon = \frac{f_\epsilon}{\|I_\epsilon\|} \to 0 \quad \tilde{I}_\epsilon = \|\frac{I_\epsilon}{\|I_\epsilon\|}\| = 1, \quad \mu\partial_t \frac{I_\epsilon}{\|I_\epsilon\|} + (\frac{I_\epsilon}{\|I_\epsilon\|} - \frac{1}{2}\int_{-1}^1 \frac{I_\epsilon}{\|I_\epsilon\|}d\mu) = \frac{f_\epsilon}{\|I_\epsilon\|} \to 0. \tag{35}$$

Now $\tilde{I}_\epsilon$ converge *weakly* to a limit solution of the Milne problem with zero data, hence to 0 by the uniqueness of the solution; To complete (by contradiction) the proof one has to show the *strong* convergence of $\tilde{I}_\epsilon$ which is of norm 1 . This follows from the so called *averaging lemma* (cf [11] and [8]) using the estimate.

$$\|\mu\partial_t \tilde{I}_\epsilon\| \leq \|(\frac{I_\epsilon}{\|I_\epsilon\|} - \frac{1}{2}\int_{-1}^1 \frac{I_\epsilon}{\|I_\epsilon\|}d\mu)\| + O(\epsilon) \tag{36}$$

7

**Proof of the non negativity**

Estimates and positivity can be deduced by the following standard intuitive arguments.

Denote by $(x_+, \mu_+)$ (resp. $(x_-, \mu_-)$ the point where $I_\epsilon$ achieves its maximum (resp minimum). Then whenever the maximum (resp. minimum) is reached inside the open set $(0, H) \times (-1, 1)$ one has:

$$\mu \partial_x I_\epsilon = 0 \,, (I_\epsilon - \frac{1}{2} \int_{-1}^{1} I_\epsilon(x\mu')d\mu')(x_+, \mu_+) \geq 0 \quad \text{resp.} \quad (I_\epsilon - \frac{1}{2} \int_{-1}^{1} I_\epsilon(x\mu')d\mu')(x_-, \mu_-) < 0 \qquad (37)$$

And if it is reached on the boundary $\Sigma_+$ one has:

$$(\mu \partial_x I)(x_+, \mu_+) \geq 0 \quad \text{resp.} \quad (\mu \partial_x I)(x_-, \mu_-) \leq 0 \,. \qquad (38)$$

Consequently, the equation:

$$\epsilon I_\epsilon + \mu \partial_x I_\epsilon + I_\epsilon - \frac{1}{2} \int_{-1}^{1} I(x, \mu')d\mu' = f(x, \mu) \qquad (39)$$

implies that if the data $f, g_0$ and $g_H$ are non negative $(37)$ if the minimum is reached inside the domain it cannot be negative. Hence if reached on the boundary by $(39)$ it cannot also be negative if reached on $\Sigma_+$. The only remaining case is the situation where this minimum is reached on $\Sigma_-$ but then it coincides with $g_0$ or $g_H$ which both are non negative. And in any case one has

$$I_\epsilon(x, \mu) \geq I_\epsilon(x_-, \mu_-) \geq 0 \qquad (40)$$

In the same way for the solutions of the problem

$$\epsilon I_\epsilon + \mu \partial_x I_\epsilon + I_\epsilon - \frac{1}{2} \int_{-1}^{1} I_\epsilon(x, \mu')d\mu' = 0, \qquad (41)$$

$$\text{with} \quad g_0(\mu) \geq 0 \quad \text{and} \quad g_H(\mu) \geq 0 \qquad (42)$$

a positive maximum cannot be reached inside the domain because with $(41)$ it should be negative which contradict $(42)$ , and it cannot be reached on $\Sigma_+$ by the same argument since $I$ coincides with $g_0(\mu)$ or $g_H(\mu)$. Since the above properties are independent of $\epsilon$ the proof of the positivity and of the estimate $(23b)$ follows by letting $\epsilon \to 0$. □

To conclude this section it is convenient to recall the implicit formula for the solution of the problem :

**Proposition 3** *Let* $J(x) = \frac{1}{2} \int_{-1}^{1} I(x, \mu)d\mu$. *The solution of* $(22)$ *with* $(21)$ *satisifies*

$$I(x, \mu) = \mathbf{1}_{\mu > 0}\Big( \frac{1}{\mu} e^{-\frac{x}{\mu}} g_0(\mu) + \int_0^x e^{-\frac{x-s}{\mu}} (J(s) + f(s, \mu)) \frac{ds}{\mu} \Big)$$
$$+ \mathbf{1}_{\mu < 0}\Big( \frac{1}{|\mu|} e^{-\frac{H-x}{|\mu|}} g_0(\mu) + \int_H^x e^{-\frac{H-x}{|\mu|}} (J(s) + f(s, \mu)) \frac{ds}{|\mu|} \Big). \qquad (43)$$

This formula under different variants will be used below.

## 4.1 Milne Problem and non explicit formula for the temperature of the earth

In $(0, H) \times (-1, 1)$ one considers an intensity of radiation $I$, coming in the domain to the earth surface from the high atmosphere i.e. for $x = 0$ and $0 < \mu < 1$ with intensity $I(0, \mu) = \mu I$ and one assumes that the albedo of the earth (i.e. the radiative intensity in term of the incoming intensity) is given in weighted Sobolev spaces by

$$\mathcal{A} : L^2(\mu^{\frac{1}{2}}, (0, 1)) \mapsto L^2(|\mu|^{\frac{1}{2}}, (0, 1)), \qquad \|\mathcal{A}(g_1) - L(g_2)\| \leq C\|g_1 - g_2\| \qquad (44)$$

where

$$\mu \partial_x I + I - \frac{1}{2} \int_{-1}^{1} I(x, \mu')d\mu' = 0, \quad I(0, \mu)|_{\mu > 0} = g(\mu)I_{sol}, \quad I(H, \mu)|_{\mu < 0} = \mathcal{A}(I(H, -\mu)) \qquad (45)$$

8

has for $C \leq 1$ a unique well defined solution (easy for $C < 1$, more subtle but as above for $\epsilon = 0$.)

The construction is done as follow:

Consider in $(0, H) \times (-1, 1)$ the unique well defined solution $I_{g,X}$ of the equation

$$\mu \partial_x I + I - \frac{1}{2} \int_{-1}^1 I(x, \mu') d\mu' = 0 \tag{46}$$

with the incoming boundary data

$$I_{g,X}(0, \mu) = g(\mu) \text{ for } \mu > 0 \text{ given and } I_{g,X}(H, \mu) = X(\mu) \text{ unknown for } \mu < 0. \tag{47}$$

Then the mapping $X \mapsto I_{g,X}(H, \mu)_{|\mu > 0}$ is affine and continuous from $L^2(|\mu|^{\frac{1}{2}}, (-1, 0))$ to $L^2(\mu^{\frac{1}{2}}, (0, 1))$ and the solution of the albedo problem is given by the following equation:

$$\text{Find } Z \in L^2(\mu^{\frac{1}{2}}, (0, 1)) \text{ such that } I_{g,\mathcal{A}(Z)}(H, \mu) = Z(\mu) \tag{48}$$

which with the hypothesis $C < 1$ has a unique solution.

The computation of the temperature follows from the Stefan-Boltzmann law.

$$\sigma T^4 = \frac{1}{2} \int_{-1}^0 \mathcal{I}_{g,\mathcal{A}(Z)}(H, \mu) d\mu + \frac{1}{2} \int_0^1 Z(\mu) d\mu d\mu \tag{49}$$

The formula (49) is perfectly well defined but far from explicit, so in need of a relevant approximation. One of the main tool for such an approximation is the introduction of the *half space Milne problem* and this is justified by the fact that after rescaling the analysis is done for $x \in (0, H)$ with $H$ large.

# 5 The Half space Milne problem

For the Milne equation, defined in $(0, H) \times (-1, 1)$,

$$\mu \partial_x I + I - \frac{1}{2} \int_{-1}^1 I(x; \mu') d\mu' = 0 \tag{50}$$

one has

$$\frac{d}{dx} \Phi_I(x) = 0 \quad \text{and} \quad \frac{d}{dx} \int_{-1}^1 \mu^2 I(x; \mu') d\mu' = \Phi_I := \Phi_I(x) = \int_{-1}^1 \mu I(x; \mu') d\mu' \tag{51}$$

where $\Phi_I$ is the flux of of $I$ which by the above observation turns out to be constant. As a consequence to remain uniformly bounded with respect to $x$ for $H \to \infty$ any solution of (50) has to have $\Phi_I = 0$. This justifies the following (cf.([5] and [6])

**Theorem 2** *For any incoming data $g_0(\mu)$ defined for $x = 0$ and $\mu \in (0, 1)$ with $\mu^{\frac{1}{2}} g_0(\mu) \in L^2(0, 1)$, there exists a unique uniformly bounded in $x$ solution of the "half space "Milne problem:*

$$\mu \partial_x I + I - \frac{1}{2} \int_{-1}^1 I(x, \mu') d\mu' = 0, \quad I(0, \mu)|_{\mu > 0} = g_0(\mu). \tag{52}$$

*This solution has $0$ flux and satisfies the estimates:*

$$\sup_{x \geq 0, \mu \in (-1,1)} |I(x, \mu)| \leq \sup_{\mu \in (0,1)} |g_0(\mu)| \quad \text{and } \forall \alpha \in [0, 1), \int_0^\infty e^{\alpha x} \int_{-1}^1 (I - \frac{1}{2} \int_{-1}^1 I)^2 d\mu' \leq \frac{1}{1-\alpha} \int_0^1 \mu |g(0, \mu)|^2 d\mu.$$

$$\tag{53}$$

*Moreover this solution converges exponentially fast to a constant $C(g_0)$; the while the mapping $g \mapsto C(g)$ is linear continuous from the space of function with $|\mu|^{\frac{1}{2}} g \in L^2(0, 1)$ into $\mathbb{R}$.*

*Proof.* Once again the proof is only sketched below; for details see [6]. First one considers the solution on a "double" space interval $(0, 2H)$ with as incoming boundary data for $x = H$ $\mu < 0 \Rightarrow I(2H, \mu) = g_0(-\mu)$ this makes the, unique well defined in $(0, 2H) \times (-1, 1)$, solution of the problem

$$\mu \partial_x I + I - \frac{1}{2} \int_{-1}^{1} I(x, \mu') d\mu' = 0 \tag{54}$$

symmetric with respect to $H$ : $\forall \{|z| < H, \mu \in (-1, 1)\}$ $I(H - z, \mu) = I(H + z, -\mu)$. Henc e for $x = H, \Phi_I(H) = \int_{-1}^{1} \mu I(H, \mu) d\mu = 0$.

Since $\Phi(x)$ is independent of $x$, it is equal to 0 everywhere.

Then the decomposition of $I$ into its average $I_a(x) = \frac{1}{2} \int_{-1}^{1} I(x, \mu') d\mu'$ and the orthogonal complement $I_{ort} = I - \frac{1}{2} \int_{-1}^{1} I(x, \mu') d\mu'$ gives, with the 0-flux property, the relation:

$$\int_{-1}^{1} \mu I^2(x, \mu) d\mu = \int_{-1}^{1} (I(x, \mu) - \frac{1}{2} \int_{-1}^{1} I(x, \mu') d\mu')^2 d\mu \tag{55}$$

Multiplying the equation by $e^{\alpha x} I$ with $0 < \alpha < 1$ and integrating on $(0, H) \times (0, 1)$ with the relation:

$$e^{\alpha x} \int_{-1}^{1} (\mu \partial_x I) I d\mu = \partial_x (e^{\alpha x} \frac{1}{2} \int_{-1}^{1} \mu I^2 d\mu)) - \alpha e^{\alpha x} \frac{1}{2} \int_{-1}^{1} \mu I^2 d\mu. \tag{56}$$

Thus, one obtains the estimate:

$$(1 - \alpha) \int_{0}^{H} e^{\alpha x} \int (I(x, \mu) - \frac{1}{2} \int_{-1}^{1} I(x, \mu') d\mu')^2 d\mu) dx \leq \int_{0}^{1} \mu |g_0(\mu)|^2 d\mu. \tag{57}$$

Returning to the equation,

$$\mu \partial_x I = -I(x, \mu) - \frac{1}{2} \int_{-1}^{1} I(x, \mu') d\mu' \tag{58}$$

gives the exponential convergence to a constant $C(g)$ for $H \to \infty$.

The uniqueness of the solution is based on the same type of estimates. $\qquad \square$

**Remark 4** *The determination of the function $g \mapsto C(g)$ in particular before the appearance of large scale computers and in the quest for an explicit or semi explicit formula has been in the last century the object of an intensive activities involving in particular Wiener Hopf calculus (cf. [7]). However the most explicit form this computation is based on the introduction of the Chandrasekhar function. A function defined by the implicit formula:*

$$H(\mu) = 1 + \frac{1}{2} \mu H(\mu) \int_{0}^{1} \frac{H(\mu')}{\mu + \mu'} d\mu' \tag{59}$$

*which gives the constant $C(g)$ by the relation*

$$C(g) = \frac{\sqrt{3}}{2} \int_{0}^{1} \mu' H(\mu') g(\mu') d\mu'. \tag{60}$$

*In particular for $g(\mu) = \mu$ one has $C(g) = \overline{\omega_1} = 0.7014$.*

## 5.1 Approximate determination of the temperature on earth

We present two approximations which yield the same formula for earth's temperature based on the asymptotic behaviour of the half-space Milne problem.

### 5.1.1 Using Theorem 2

We return to the notations used in [9] for climate dynamics: $\tau = 1 - e^{-r}$ where $r$ is the altitude; $H$ is the thickness of the atmosphere and $Z = 1 - e^{-H}$. One observes that the formula $\tilde{I} = (\mu - \tau)$ provides a solution of the Milne equation for $\tau \in \mathbb{R}$ with constant flux given by

$$\tilde{\Phi} = \int_{-1}^{1} \mu(\tau - \mu)d\mu = -\frac{2}{3} \tag{61}$$

Hence one introduce the solution $e(\tau, \mu)$ of the half space problem with 0 flux and equal to $\mu$ at $\tau = 0$ for $\mu > 0$ . As was proven in the theorem 2 such solution exists is unique and converges exponentially fast to the constant $\overline{\omega_1}$ as $\tau$ goes to $\infty$ . As such

$$I = c[\tau - \mu + \mathrm{rem}(\tau, \mu)] \tag{62}$$

provides a *boundary layer approximation* (ie for $\tau > 0$ not far from 0) of the solution of the Milne problem with a flux given equal to $\frac{2}{3}c$ no incoming density for $\tau = 0$ and $\mathrm{rem}(\tau, \mu)$ going exponentially fast to $\overline{\omega_1}$ when $\tau \to 1$. Hence for $H$ large enough one has

$$\text{For } \mu < 0 \ I(0, \mu) = c[-\mu + \overline{\omega_1}] + o(e^{-\alpha H}) \tag{63}$$

Therefore for $\tau = 0$

$$\int_{-1}^{1} I(0, \mu))d\mu \simeq c \int_{-1}^{0} ((-\mu) + \overline{\omega_1})d\mu = \frac{c}{2} + c\overline{\omega_1} \tag{64}$$

For a solar flux equal to $\Phi$ the intensity $I_{earth}$ is obtained after be multiplication by $\frac{3}{2}\Phi$ (see (61). This gives:

$$\int_{-1}^{1} I_{earth}(\mu)d\mu \simeq \frac{3}{4}\Phi(1 + 2\overline{\omega_1}) \tag{65}$$

and with the Stephan Boltzmann law one obtains:

$$T_{earth} \simeq \left(\frac{3}{8\sigma}\Phi(1 + 2\overline{\omega_1})\right)^{\frac{1}{4}} \tag{66}$$

### 5.1.2 Using an approximation of the Schwarzfield solution

In Appendix B of Fowler [9], a semi-analytic solution of the Milne problem is given in terms of a complex integral. It is said also that (notice the similarity with what has been written above)

$$\bar{I} = 1.3 - (Z - \tau) - \mu - \mathbf{1}_{\mu>0}(1.3 - \mu)e^{-\frac{(Z-\tau)}{\mu}} \tag{67}$$

Figure 3 displays (on the left) $I(\tau, \mu)$ given by (67). For comparison a numerical soultion of the Milner problem (see below) is shown on the right in the same figure. The plots don't agree because the boundary conditions are not (and cannot be) the same, but the general trend is the same. The numerical method presented below corresponding to the right plot in figure 3, gives a temperature on earth $T = 293K$. Formula (66) with $\Phi = Q(1-a)/4$ as in [9] eq (1.18) p66, gives $T = 351K$.

## 6 Numerical Analysis

Consider (19), adimentionalised :

$$\mu\frac{\partial I_\nu}{\partial \tau} + \gamma(\tau, \mu)\frac{\partial I_\nu}{\partial \mu} + \kappa_\nu (I_\nu - B_\nu(T)) = 0, \ \forall \{\tau, \mu\} \in (0, Z) \times (-1, 1), \forall \nu \in \mathbb{R}^+, \tag{68}$$

$$B_\nu(T) = \frac{\nu^3}{e^{\frac{\nu}{T}} - 1}, \quad \int_0^\infty \kappa_\nu \left(B_\nu(T) - \frac{1}{2}\int_{-1}^{1} I_\nu d\mu\right) d\nu = 0, \ \forall \tau \in (0, Z), \tag{69}$$

$$I_\nu(Z, \mu) = 0, \ \forall \mu < 0, \quad I_\nu(0, \mu) = \mu Q_\nu, \ \forall \mu > 0, \tag{70}$$
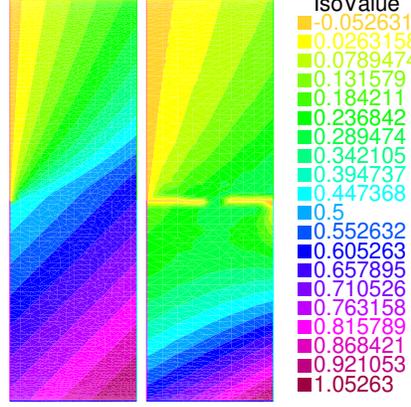
Figure 3: Semi-analytical solution (left) and numerical solution (right) based on (73). Color intensity plots in the rectangle $\tau, \mu \in (0,1) \times (0,2)$. The differences are due to the different boundary conditions: a flux condition for the one on the left and a Dirichlet condition on $\Sigma_-$ for the one on the right. One sees also on the plots the singularities of the integrands at $\mu = 0$: a red spot on the left plot and a yellow line on the right.

The physical constants are given in Table 1. Following (14)(15), we set $\nu_0 = 10^{14}$ so that $\nu \in (0.01, 20)$, choose $B_0 = \frac{2\hbar\nu_0^3}{c^2} = 1.47\,10^{-8}$ and $T_0 = \frac{\hbar\nu_0}{k}$, then the physical quantites (noted with a tilde) are recovered by $\tilde{T} = T_0 T$, $\tilde{B}_\nu(T) = B_0 B_\nu(T)$, $\tilde{I}_\nu = B_0 I_\nu$. Similarly we choose $\lambda = 10^3$ and set $\kappa_\nu = \lambda \rho_0 \tilde{\kappa}_\nu = 1.225 \tilde{\kappa}_\nu$. Thus, in the computation $H = 12$ and $R = 40000$; but $R$ does not appear if the Chandraskhar correction is neglected.

The energy of the sun light is $1370\mathrm{Wm}^{-2}$, so, at the equator $\cos\theta = 1$, with $a = 0.3$, $Q_0 = 1370(1-a) = 959$, giving $Q_\nu = 1.397\,10^{-5} B_\nu(T_{sun})$ .

If $\kappa_\nu$ is independent of $\nu$ then $\bar{I} = \int_0^\infty I_\nu \mathrm{d}\nu$ may be computed with $Q_\nu = 1$ and then $T$ is given by

$$T(\tau) = \left( \frac{Q_0}{2\sigma_b} \int_{-1}^{1} I(\tau, \mu) \mathrm{d}\mu \right)^{\frac{1}{4}} \tag{71}$$

Table 1: *The physical constants.*

| $c$ | $\hbar$ | $k$ | $\rho_0$ | $R$ | $H$ | $\sigma_b$ |
|---|---|---|---|---|---|---|
| $2.998\,10^8$ | $6.6261\,10^{-34}$ | $1.381\,10^{-23}$ | $1.225\,10^{-3}$ | $4\,10^7$ | $12\,10^3$ | $1.801\,10^{-8}$ |

## 6.1   Numerical scheme

The numerical scheme is based on the observation that the solution of (68)-(70) with $T \mapsto B_\nu(T)$ given, is

$$I_\nu = \mathbf{1}_{\mu>0} \left[ \mu e^{-\kappa_\nu \frac{\tau}{\mu}} + \int_0^\tau \frac{e^{\kappa_\nu \frac{t-\tau}{\mu}}}{\mu} B_\nu(t) \mathrm{d}t \right] - \mathbf{1}_{\mu<0} \int_\tau^Z \frac{e^{\kappa_\nu \frac{t-\tau}{\mu}}}{\mu} B_\nu(t) \mathrm{d}t. \tag{72}$$

**Example**   $B = \mu \;\Rightarrow\; I_\nu = \mathbf{1}_{\mu>0} \left[ \mu(1 + \frac{1}{\kappa_\nu}) e^{-\kappa_\nu \frac{\tau}{\mu}} - \frac{\mu}{\kappa_\nu} \right] - \mathbf{1}_{\mu<0} \left[ \frac{\mu}{\kappa_\nu} (1 - e^{\kappa_\nu \frac{(Z-\tau)}{\mu}}) \right].$

Programming (72) is straightforward; it needs only to be evaluated at all vertices of a triangulation of the rectangle $\Omega$. Table 2 shows the error versus the mesh size for the above example. Note however that the precision is weak: $O(h)$, probably because the solution is singular at $\mu = 0$.

Alternatively , following [21], a finite element method has been tested. It uses a weak formulation of (68) discretized with Lagrangian-$P^1$ triangular elements For stability a least square upwinding term (SUPG) is added, namely $h_{\mathrm{SUPG}}(\mu\partial_\tau I + \kappa_\nu I)(\mu\partial_\tau \hat{I} + \kappa_\nu \hat{I})$ for a small $h_{\mathrm{SUPG}}$, where $\hat{I}$ is the test function of the variational formulation. The performance of the method is reported in Table 2. It appears to be less efficient than (72), but faster. The results could be sensitive to values chosen for $h_{\mathrm{SUPB}}$.

Table 2: Numerical error versus mesh size $h$ on Example 1: the error is $O(h)$

| Number of Vertices | 1107 | 4008 | 9856 |
|---|---|---|---|
| $L^2$-error by FEM | $20.\,10^{-4}$ | $7.7\,10^{-4}$ | $3.7\,10^{-4}$ |
| $L^2$-error by (72) | $14\,10^{-4}$ | $0.45\,10^{-4}$ | $0.12\,10^{-4}$ |

## 6.2 The Milne problem

To solve the Milne problem, we use the following iterations, initialized with $B^0(\cdot) \equiv 0$:

$$I^{n+1} = \mathbf{1}_{\mu>0}\left[\mu e^{-\kappa\frac{\tau}{\mu}} + \int_0^\tau \frac{e^{\kappa\frac{t-\tau}{\mu}}}{\mu}B^n(t)\mathrm{d}t\right] - \mathbf{1}_{\mu<0}\int_\tau^Z \frac{e^{\kappa\frac{t-\tau}{\mu}}}{\mu}B^n(t)\mathrm{d}t, \quad B^{n+1}(\tau) = \frac{1}{2}\int_{-1}^1 I^{n+1}\mathrm{d}\mu. \qquad (73)$$

### 6.2.1 Convergence of the iterative scheme

For clarity let $\kappa = 1$. Scheme (73) is a numerical implementation of the following iterations:

$$\mu\partial_\tau I^{n+1} + (1+\varepsilon)I^{n+1} = \frac{1}{2}\int_{-1}^1 I^n\mathrm{d}\mu$$

Adding the terms with $\epsilon$ makes the convergence proof rather simple. Indeed,

$$\mu\partial_\tau(I^{n+1} - I^n) + (1+\varepsilon)(I^{n+1} - I^n) = \frac{1}{2}\int_{-1}^1 (I^n - I^{n-1})\mathrm{d}\mu$$

Consequently,

$$\int_\Omega \frac{\mu}{2}\partial_\tau(I^{n+1} - I^n)^2 + (1+\varepsilon)\int_\Omega(I^{n+1} - I^n)^2 = \int_\Omega(I^{n+1} - I^n)(I^n - I^{n-1})$$

$$\Rightarrow \quad \int_{-1}^1 \mu|I^{n+1} - I^n|^2(\tau,\mu)\mathrm{d}\mu\Big|_0^Z + (1+\varepsilon)\|I^{n+1} - I^n\|_{0,\Omega}^2 \le \|I^{n+1} - I^n\|_{0,\Omega}\|I^n - I^{n-1}\|_{0,\Omega}$$

$$\Rightarrow \quad \|I^{n+1} - I^n\|_{0,\Omega} \le \frac{1}{(1+\varepsilon)}\|I^n - I^{n-1}\|_{0,\Omega} \le \frac{1}{(1+\varepsilon)^n}\|I^1 - I^0\|_{0,\Omega}$$

### 6.2.2 Results

In practice the convergence is much faster than predicted above, as shown by Table 3. A typical result is also shown, in the physical coordinates, on figure 4. The right side of figure 3 shows the solution of Milne's problem computed on a grid $40 \times 20$. The temperature on earth given by (71) is $T = 293K$.

13

Table 3: Convergence of the fixed point algorithm with $\kappa_\nu = 1$.

| Iteration | 1 | 2 | 3 | 4 | 5 |
|---|---|---|---|---|---|
| $\|I^{n+1} - I^n\|_0^2$ | 0.524721 | 0.0315412 | 0.00777077 | 0.00188975 | 0.000457752 |
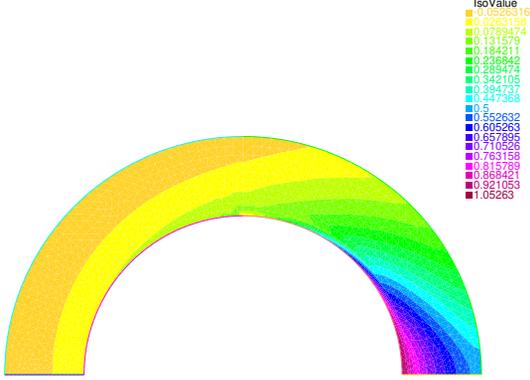


Figure 4: Light intensity level map in the physical domain, i.e. for all $\phi$ and $r$. Even though the cercle has radius $R$, this is not a plot on a cross section of the planet. It shows $I(r,\phi)$ for $r \in (0,H)$ and $\phi \in (-\pi, \pi)$.
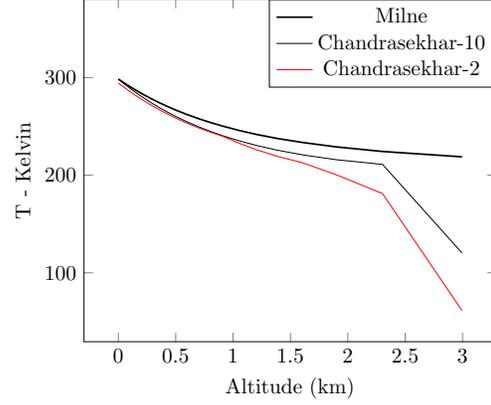


Figure 5: Temperature computed with the Milne and Chandrasekhar equations. In the later case the earth radius is 2 or 10 times the atmosphere thickness.

## 6.3 The Chandrasekhar equation

For a grey atmosphere the model with the Chandrasekhar correction reduces to

$$\frac{1}{\kappa}\mu\partial_\tau I + I + \gamma(\tau,\mu)\partial_y I = \frac{1}{2}\int_{-1}^1 I \mathrm{d}y, \quad \forall \tau, \mu \in \Omega \coloneqq (0,Z) \times (-1,1) \tag{74}$$

and (11). The following numerical scheme is used:

$$\cdot\ B^n(\tau) = \frac{1}{2}\int_{-1}^1 I^n(\tau,\mu)\mathrm{d}\mu,$$
$$\cdot\ I^{n+\frac{1}{2}} = \mathbf{1}_{\mu>0}\left[\mu e^{-\kappa\frac{\tau}{\mu}} + \int_0^\tau \frac{e^{\kappa\frac{t-\tau}{\mu}}}{\mu}B_\nu^n(t)\mathrm{d}t\right] - \mathbf{1}_{\mu<0}\int_\tau^Z \frac{e^{\kappa\frac{t-\tau}{\mu}}}{\mu},$$
$$\cdot\ I^{n+1} + \gamma\partial_\mu I^{n+1} = I^{n+\frac{1}{2}}, \text{ in } \Omega \text{ with boundary conditions (11)}. \tag{75}$$

This scheme is consistent because $I^{n+\frac{1}{2}}$ satisfies $\frac{\mu}{\kappa}\partial_\tau I^{n+\frac{1}{2}} + I^{n+\frac{1}{2}} = B^n$ and adding this to the last equation above gives $I^{n+1} + \gamma\partial_\mu I^{n+1} + \frac{\mu}{\kappa}\partial_\tau I^{n+\frac{1}{2}} = B^n$.

Assuming (unrealistic) regularity, the last equation of the scheme is written in weak form in the space

$$V = \{v \in H^1(\Omega) : v(Z,\mu) = 0 \ \forall \mu < 0, \ v(0,\mu) = 0, \forall \mu > 0, \forall \tau \in (0,Z)\}$$

with additional artificial viscosity of amplitude $\delta$ and SUPG: find $I$ with (11) and, for all $\hat{I} \in V$,

$$\int_\Omega \left(I^{n+1} + \gamma\partial_\mu I^{n+1}\right)\hat{I} + \int_\Omega \frac{\delta}{2}\left(|\mu|\partial_\tau I\partial_\tau \hat{I} + |\gamma|\partial_\mu I\partial_\mu \hat{I}\right) + \int_\Omega h_{\mathrm{SUPG}}(\mu\partial_\tau I + \kappa_\nu I)(\mu\partial_\tau \hat{I} + \kappa_\nu \hat{I}) = \int_\Omega I^{n+\frac{1}{2}}\hat{I}.$$

When the above is discretized by a $P^1$ Finite Element Method, the convergence of the fixed point algorithm is equaly fast, as shown by Table 4; results are shown on figures 7 and 10 and illustrate the convergence f the Chandrasekhar equations to the Milne equation when $R$ increases.

Figure 6: Light Intensity plotted in the physical domain when $R = 2.4, H = 1.2$ and $R = 24, H = 1.2$

# 7 Numerical simulation of the greenhouse effect

The problem is defined in (68),(69),(70).

As the sun temperature is around $5700K$, sunlight frequencies are in the range $\nu \in (0.5, 15)10^{14}$ with a maximum around 6; the earth temperature being around 300K, its infrared response is in the range $\nu \in (0.01, 0.5)10^{14}$ with a maximum at 0.16 (see the right part of figure 7). With $\nu_0 = 10^{14}$, the reduced temperatures are $T_e = 300k/(\hbar\nu_0) = 0.06$, $T_s = 5700k/(\hbar\nu_0) = 1.18$ for earth and sun.

With $B_0 = c^2/(2h\nu_0^3)$ as in (14), we set $Q_\nu(T) = 1.395\,10^{-5}\nu^3/(e^{\frac{\nu}{T}} - 1)$ and the computer simulations give a reduced temperature for earth around 0.07. The Boltzmann functions for earth and sun are shown on 7.

Our aim is to compare the earth surface temperature for two different functions $\nu \to \kappa_\nu(\nu)$ and what counts is the relative change of temperature obtained. The functions $\kappa(\nu)$ are greater than 1 because of the rescaling $\lambda\rho_0\rho\kappa_\nu$ with $\lambda\rho_0 = 1$ :

$$\kappa_\nu^1 \equiv 0.8 \text{ and } \kappa_\nu^2 = 0.8 + \delta\kappa \mathbf{1}_{\nu\in(\nu_1,\nu_2)}. \tag{76}$$

with $\nu_1 = 0.07$, $\nu_2 = 0.09$ and $\delta\kappa = 0.25$ or $0.5$.

Finding $T$ by inverting the Planck function can be challenging. A fairly accurate approximation can be found as follows: When $\kappa_\nu = \kappa$ is constant finding $T^*$ by inverting the Planck function, is easier because.

$$\int_0^\infty \kappa.B_\nu(T^*) = \kappa \int_0^\infty \frac{\nu^3}{e^{\frac{\nu}{T^*}} - 1} = \kappa\frac{\pi^4}{15}T^{*4}, \Rightarrow T^* \approx \frac{1}{\pi}\left(\int_{\nu_m}^{\nu_M} \frac{15}{2\kappa} \int_{-1}^1 \kappa_\nu I_\nu \mathrm{d}\mu d\nu\right)^{\frac{1}{4}}. \tag{77}$$

The following numerical scheme is used:

. Set $K_I{}^0 = 0$,

**for** ( $\nu = \nu_m; \nu < \nu_M; \nu+ = \delta\nu$){

. Compute $\tau \mapsto T^n(\tau)$ by $T^n = \frac{1}{\pi}\left(\frac{15}{2\kappa_\nu^1} \int_{-1}^1 K_I \mathrm{d}\mu\right)^{\frac{1}{4}}$ ; then

. **for**($\nu = \nu_m; \nu < \nu_M; \nu+ = \delta\nu$){

. $B_\nu^n(t) = \frac{\nu^3}{e^{\frac{\nu}{T^n(t)}} - 1}$,

15

Figure 7: Plot of $B_\nu(T) = \frac{B\nu^3}{e^{\frac{\nu}{T}}-1}$ representing the Light intensities versus $\nu$ expected relevant to the numerical simulations, except that $B_\nu(0.06)$ being too stiff, we used $B_\nu(0.2)$. $B_\nu(1.18)$ corresponds to sunlight.

Figure 8: Temperature computed by solving the Milne problem (solid curves) compared with the solution obtained with algorithm (78) with $\kappa_\nu$ constant (dashed curves). Convergence is shown with respect to $n$ which controls the number of vertices of the mesh, (proportional to $n^2$).

$$
\begin{aligned}
& . \quad I_\nu^{n+\frac{1}{2}} = \mathbf{1}_{\mu>0}\left[\mu Q_0 B_\nu(T_{sun})e^{-\kappa_\nu \frac{\tau}{\mu}} + \int_0^\tau \frac{e^{\kappa_\nu \frac{t-\tau}{\mu}}}{\mu}B_\nu^n(t)\mathrm{d}t\right] - \mathbf{1}_{\mu<0}\int_\tau^Z \frac{e^{\kappa_\nu \frac{t-\tau}{\mu}}}{\mu}B_\nu(t)\mathrm{d}t, \\
& . \quad I_\nu^{n+1} + \gamma\partial_\mu I_\nu^{n+1} = I_\nu^{n+\frac{1}{2}}, \text{ with boundary conditions (11),} \\
& . \quad {K_I}^{n+1} + = \kappa_\nu I_\nu^{n+1}\delta\nu. \\
& \quad \} \\
& \} 
\end{aligned}
\tag{78}
$$

To assert the method we ask algorithm (78) to recover the solution of the Milne problem ($\kappa_\nu$ constant). The results are shown on figure 8. Both curves coincide when the Finite Element Method is used; with the semi-analytic formula, it fails because the formula looses additivity with respect to $B_\nu$. Figure 8 also shows convergence when the mesh is refined by the factor $n$.

Then we computed the relative change of temperature when $\kappa_\nu$ is changed from $\kappa_\nu^1$ to $\kappa_\nu^2$. The change is of the order of $10^{-3}$ and negative (see figure 10). This computer implementation however is not capable of computing a realistic change when $\kappa_\nu$ is modified in such a small frequency window. Hence we turned to calculus of variation.

## 7.1 Solution by calculus of variations

Let $\nu_2 - \nu_1$ be small, and let (76) be written as $\kappa_\nu = \kappa + \delta\kappa_\nu$ with $\delta k_\nu = 0$ if $\nu \notin (\nu_1, \nu_2)$. With the obvious notations of a calculus of variations:

$$
\mu\partial_\tau \delta I_\nu + \kappa\delta I_\nu = \kappa\delta B_\nu + \delta\kappa_\nu(B_\nu - I_\nu), \quad \delta I_\nu(0,\mu)|_{\mu>0} = \delta I_\nu(Z,\mu)|_{\mu<0} = 0,
$$
$$
\int_0^\infty (\delta B_\nu - \frac{1}{2}\int_{-1}^1 \delta I_\nu \mathrm{d}\mu)\kappa \mathrm{d}\nu = -\int_0^\infty (B_\nu - \frac{1}{2}\int_{-1}^1 I_\nu \mathrm{d}\mu)\delta\kappa_\nu \mathrm{d}\nu
\tag{79}
$$

Let $\delta\bar{I} = \int_0^\infty \delta I_\nu \mathrm{d}\nu$ and similarly for $\delta\bar{B}$. Integrating the first equation leads to

$$
\mu\partial_\tau \delta\bar{I} + \kappa\delta\bar{I} - \kappa\delta\bar{B} = \int_{\nu_1}^{\nu_2} \delta\kappa_\nu(B_\nu - I_\nu)\mathrm{d}\nu, \quad \delta\bar{I}(0,\mu)|_{\mu>0} = \delta\bar{I}(Z,\mu)|_{\mu<0} = 0,
\tag{80}
$$

$$
\kappa\left(\delta\bar{B} - \frac{1}{2}\int_{-1}^1 \delta\bar{I}\mathrm{d}\mu\right) = -\int_{\nu_1}^{\nu_2}\left(B_\nu - \frac{1}{2}\int_{-1}^1 I_\nu \mathrm{d}\mu\right)\delta\kappa_\nu \mathrm{d}\nu
\tag{81}
$$

16

Figure 9: Color map of $\delta I$, when $\delta \kappa = 0.25 \mathbf{1}_{\nu \in (0.02, 0.04)}$, the solution of (82). Colors are plotted in the physical domain $r, \phi$. It indicates that infrared rays intensity changes are negative for rays in the direction of the sun and positive in the opposite direction.
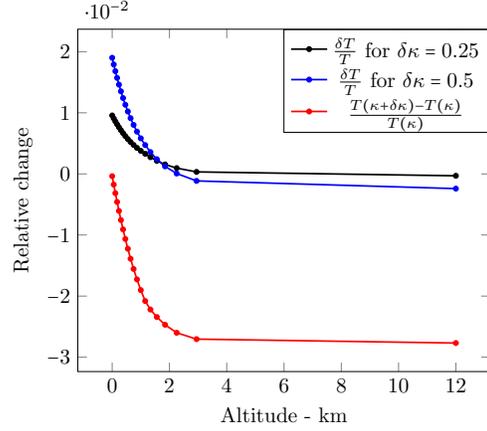
Figure 10: Relative temperature change versus altitude, computed with $\kappa_\nu = 0.8 + \delta \kappa \mathbf{1}_{\nu \in (0.02, 0.04)}$ and $\delta \kappa = 0.25$ or $0.5$ to account for the greenhouse gas opacity (see (83)). A direct computation of the relative changed is also displayed for $\delta \kappa = 0.25$.

Adding both gives

$$\mu \partial_\tau \delta \bar{I} + \kappa \delta \bar{I} - \frac{\kappa}{2} \int_{-1}^{1} \delta \bar{I} \mathrm{d}\mu = -\int_{\nu_1}^{\nu_2} \left( I_\nu - \frac{1}{2} \int_{-1}^{1} I_\nu \mathrm{d}\mu \right) \delta \kappa_\nu \mathrm{d}\nu \tag{82}$$

and, knowing that $\delta B = \delta\left(\frac{\pi^4 T^4}{15}\right) = 4 \frac{\pi^4 T^3}{15} \delta T$, the change in temperature is computed by (81) divided by $\kappa$:

$$\frac{4\pi^4 T^3}{15} \delta T = \frac{1}{2} \int_{-1}^{1} \delta \bar{I} \mathrm{d}\mu - \frac{1}{\kappa} \int_{\nu_1}^{\nu_2} \left( B_\nu - \frac{1}{2} \int_{-1}^{1} I_\nu \mathrm{d}\mu \right) \delta \kappa_\nu \mathrm{d}\nu \tag{83}$$

The numerical results using this method are shown on figures 4 and 10. If these are to be believed, then greenhouse gases induce an increase of temperature at the earth surface of 2% (resp 4%)when $\delta \kappa = 0.25$ (resp 0.5) in the frequency range $(0.02, 0.04)10^{14}$. This computation however is polluted by the overlap of the Boltzmann function for earth and sun, the energy of the later being still larger than the infrared one. A more careful numerical investigation should be done with a full inversion of the Boltzmann function rather than using the Stefan-Boltzmann integral relation.

As the reader may want to improve this preliminary computation, we give the `FreeFem++`[22] script in appendix.

# 8 Boundary layer near the earth surface

Consider the Chandrasekhar equations with thermal diffusion: $\forall r, \mu \in (0, H) \times (-1, 1)$,

$$\mu \frac{\partial \bar{I}_\nu}{\partial r} + \frac{1 - \mu^2}{R + r} \frac{\partial \bar{I}_\nu}{\partial \mu} + \kappa_\nu \rho \left( \bar{I}_\nu - B_\nu(T) \right) = 0, \tag{84}$$

$$-\frac{\kappa_T}{(R+r)^2} \left( \partial_r ((R+r)^2 \partial_r T) + \frac{1}{1 - \eta^2} \partial_\eta^2 T \right) + \int_0^\infty \left( \rho \kappa_\nu (B_\nu(T) - \frac{1}{2} \int_{-1}^{1} \bar{I}_\nu \mathrm{d}\mu \right) d\nu = 0 \tag{85}$$

$$I_\nu(Z, \mu)|_{\mu<0} = 0, \quad I_\nu(0, \mu) = \mu Q_\nu, \quad \frac{\partial T}{\partial r}\Big|_{0, Z} = 0 \tag{86}$$

17

where $\eta = \cos\theta$ and assume that $\kappa_T = \epsilon\kappa_0$, $\epsilon << 1$. Then it is likely that

$$T = T_0 + \epsilon T_1(\frac{r}{\sqrt{\epsilon}}, \mu), \quad \bar{I}_\nu = I_0 + \epsilon I_1, \tag{87}$$

with $T_1(r, \mu) << 1$ when $r \to \infty$. This leads to the following cascade of equations

$$\mu\frac{\partial I_0}{\partial r} + \frac{1-\mu^2}{R+r}\frac{\partial I_0}{\partial \mu} + \kappa_\nu\rho\left(I_0 - B_\nu(T_0)\right) = 0, \quad B_\nu(T_0) - \frac{1}{2}\int_{-1}^{1} I_0 = 0, \tag{88}$$

$$\mu\frac{\partial I_1}{\partial r} + \frac{1-\eta^2}{R+r}\frac{\partial I_1}{\partial \mu} + \kappa_\nu\rho\left(I_1 - \partial_T B_\nu(T_0)T_1\right) = 0, \tag{89}$$

$$-\kappa_0\partial_{r'}^2 T_1 + \int_0^\infty\left(\rho\kappa_\nu(\partial_T B_\nu(T_0)T_1 - \frac{1}{2}\int_{-1}^{1} I_1\mathrm{d}\mu\right) = \frac{\kappa_0}{(R+r)^2}\left(\partial_r((R+r)^2\partial_r T_0) + \frac{1}{1-\eta^2}\partial_\eta^2 T_0\right) \tag{90}$$

with $r' = \sqrt{\frac{r}{\epsilon}}$. For clarity and without losing generality we assume $R$ is large so as to reduces the above to

$$\mu\frac{\partial I_0}{\partial r} + \kappa_\nu\rho\left(I_0 - B_\nu(T_0)\right) = 0, \quad B_\nu(T_0) - \frac{1}{4\pi}\int_{\mathbb{S}^2} I_0 = 0 \tag{91}$$

$$\mu\frac{\partial I_1}{\partial r} + \kappa_\nu\rho\left(I_1 - \partial_T B_\nu(T_0)T_1\right) = 0, \tag{92}$$

$$-\kappa_0\partial_{r'}^2 T_1(r') + T_1(r')\int_0^\infty \rho\kappa_\nu\partial_T B_\nu(T_0)d\nu = \kappa_0\partial_r^2 T_0 + \int_0^\infty \rho\kappa_\nu\frac{1}{2}\int_{-1}^{1} I_1\mathrm{d}\mu d\nu. \tag{93}$$

The last line is also $-\partial_{r'}^2 T_1 + bT_1 = c$, with $b = \frac{1}{\kappa_0}\int_0^\infty \rho\kappa_\nu\partial_T B_\nu(T_0)d\nu$ and $c = \partial_r^2 T_0 + \int_0^\infty \frac{\rho\kappa_\nu}{2\kappa_0}\int_{-1}^{1} I_1\mathrm{d}\mu d\nu$
Therefore

$$T(r) = T_0(r) + \epsilon\left(c + be^{-\sqrt{b}\frac{r}{\epsilon}}\right). \tag{94}$$

The conclusion is that there is no strong variation of the temperature $r \mapsto T(r)$ near the surface (r=0) due to thermal diffusion, but there is a strong variation of the gradient.

To connect with the next section we notice that (94) can be rewritten as:

$$\epsilon\frac{\partial(T-T_0)}{\partial r} + \sqrt{b}(T - T_0) = 0.$$

## 8.1 Boundary layer and Robin boundary condition

The temperature is a solution of an elliptic or parabolic equation ($\{x \in \Omega\}$ which requires a boundary information on $\{x \in \partial\Omega\}$ while the boundary condition for $I$ needs to be given only on the incoming part of $\Sigma_-$ of $\partial\Omega$.

Observe that (94) involves two temperatures $T_0(r)$ which could be expressed in term of $I$ by the Stephan Boltzmann law and and a temperature $T(r)$ which represent the "observed temperature" near the boundary (which is unknown ) and determined in term of non explicite constants. Such fact was already observed in nuclear reactor technology, where it leads for the diffusion approximation to a Robin boundary condition and is already explained in [13] (p.199 eq. (8.13)).

Below, following [8] and [6] we propose a self contained derivation of this type of formula based on scaling analysis. Moreover for the sake of simplicity we consider the solutions $I_\epsilon$ of a $\epsilon$ dependent half space 0-flux (cf. section 5) Milne problem; one has the following

**Proposition 4** *The family $I_\epsilon$ of solutions of the half space Milne Problem*

$$\epsilon I_\epsilon + \sqrt{\epsilon}\mu\partial_r I_\epsilon + I_\epsilon - \frac{1}{2}\int_{-1}^{1} I_\epsilon(r, \mu')d\mu' = 0, \quad I(0, \mu)|_{\mu>0} = I(0), \tag{95}$$

*converge to the $\mu$ independent solution of the diffusion equation*

$$\overline{I}_0 - \frac{1}{3}\partial_r^2 \overline{I}_0 = 0 \ \ in \ \ \mathbb{R}_r^+ \tag{96}$$

*with the Dirichlet boundary data $\overline{I}(0) = I(0)$, with a rate of convergence $O(\sqrt{\epsilon})$ in $L^2(\mathbb{R}_r^+; L^2(-1,1))$. However the expression*

$$(I_0(r) - \sqrt{\epsilon}\mu\partial_r I_0(r)) + \overline{\omega_1}\sqrt{\epsilon}\partial_r I_0(0)$$

*provides an approximation of order $\epsilon$ in $L^\infty(\mathbb{R}_t^+ \times (-1,1))$*

With standard a priori estimates as used above one observes that $I_\epsilon$ is uniformly bounded in $L^\infty(\mathbb{R}_t^+; L_\mu^\infty(-1,1))$ hence by standard estimates related to the diffusion approximation , it converges to a $\mu$ independent function $I_0(r)$ solution of the equation:

$$I_0(r) - \frac{1}{3}\partial_r^2 I_0 = 0 \quad I_0(0) = I(0) \tag{97}$$

Then one observes also that

$$\tilde{I}_\epsilon(r,\mu) = I_0(r) - \sqrt{\epsilon}\mu\partial_r I_0(r) \tag{98}$$

is a solution with an error of the order of $\sqrt{\epsilon}$ of the equation (95). This construction can be iterated giving a solution of any finite order of this equation. However at the level at $r = 0$ and $\mu > 0$ one has:

$$I(0,\mu) - \tilde{I}_\epsilon(0,\mu) = \sqrt{\epsilon}\mu\partial_r I_0(r) \tag{99}$$

and this estimation concerns a boundary layer of size $\sqrt{\epsilon}$ which can be only analyzed by the use of the zero flux solution $e(x,\mu)$ of the half space problem:

$$\mu\partial_r e + e - \frac{1}{2}\int_{-1}^1 e(r,\mu')d\mu', \quad \text{for} \ \ \mu > 0 \ \ e(0,\mu) = \mu. \tag{100}$$

Therefore one introduces the functions:

$$I_{\text{rem}}(r,\mu) = \left(\sqrt{\epsilon}\partial_r I_0(r)(e(\frac{r}{\sqrt{\epsilon}},\mu) - \overline{\omega_1}\right) + \sqrt{\epsilon}\overline{\omega_1}\partial_r I_0(r)$$
$$I_c(r,\mu) = (I_0(r) - \sqrt{\epsilon}\mu\partial_r I_0(r,\mu)) - I_{\text{rem}}(r,\mu) \tag{101}$$

Constructed in such a way $I_c(r,\mu)$ enjoys the following properties.

- It is a solution of the equation ( 95) with a reminder of order $\epsilon$.

- For $r = 0$ and $\mu > 0$ one has $I_c(r,\mu) = I_0(0)$.

- $I_{\text{rem}}$ is the sum of two terms the constant $\sqrt{\epsilon}\overline{\omega_1}\partial_r I_0(r)$ and the boundary layer term:

$$BL_\epsilon(r,\mu) = \left(\sqrt{\epsilon}\partial_r I_0(r)(e(\frac{r}{\sqrt{\epsilon}},\mu) - \overline{\omega_1}\right) \tag{102}$$

According to the theorem 2 one has: $\sup_\mu |BL_\epsilon(r,\mu)| \le C^{-\alpha\frac{r}{\epsilon}}$.

As a consequence of these observations one has

$$I_\epsilon = (I_0(r) - \sqrt{\epsilon}\mu\partial_r I_0(r)) + \overline{\omega_1}\sqrt{\epsilon}\partial_r I_0(0) + O(\epsilon) \tag{103}$$

Without going into detail we propose to deduce from the above derivation with no full proof available a the time of the writing the following

**Corollary 4** *Assume that the intensity of radiation $I_\epsilon$ of the above Milne problem is coupled with the solution of diffusion equation at the boundary of the domain by the Stephan Boltzmann relation:*

$$\sigma T_\epsilon^4 = \int_{-1}^{1} I_\epsilon(0,\mu)d\mu \tag{104}$$

*then the introduction of a Robin boundary condition of the type*

$$T_\epsilon(0) - 4\overline{\omega_1}\sqrt{\epsilon}\partial_r T_\epsilon(0) = T_0(0)\frac{T_0}{T_\epsilon} \tag{105}$$

*in the diffusion approximation will improve it from an order of $\sqrt{\epsilon}$ to $\epsilon$.*

*Proof.* Starting from the relations

$$\sigma T_c^4(r) = \frac{1}{2}\int_{-1}^{1} I(I_c(r,\mu))d\mu \quad \sigma, \quad T_0^4(r) = \frac{1}{2}\int_{-1}^{1} I(I_0(r,\mu))d\mu \tag{106}$$

one deduces from the formula (103) that

$$T^4(0) = T_0^4 + 4T_0^3\overline{\omega_1}\sqrt{\epsilon}\partial_r T_0 + O(\epsilon) \tag{107}$$

From which (observing that the exterior normal to $(0,\infty)$ is equal to $-1$ follows the Robin boundary condition.

$$T_\epsilon(0) - 4\overline{\omega_1}\sqrt{\epsilon}\partial_r T_\epsilon(0) = T_0(0)\frac{T_0}{T_\epsilon} \tag{108}$$

$\square$

# 9   Conclusion

To summerize, we may say that radiative transfer is an old topic, studied by astronomers and nuclear scientists and more recently by climate modellers. Much of the ancient material can be discarded in view of the more powerful computer solutions. However it turns out that for the simulation of the effect of sunlight on the atmosphere, the problem is numerically difficult, so that any mathematical and analytical properties gathered in the past are welcome.

Over the last fifty years the mathematical approach of subject enjoyed stimulus including a huge range of applications, and the introduction at almost the same time of the use of functional analysis and large scale computing. However one observes that there is still room for progress on the full model, in particular to make the hypothesis needed for proofs much more in agreement with the case considered in any kind of physics. As underlined above the equations (3),(4) leads to the following comments

- For sufficiently regular coefficients ($\kappa, \rho$ and regular initial and boundary data), as it is expected the problem has a unique well defined (for a finit time) , solution, which can be extended on $[0,\infty)$ when $f = 0$ (cf. [15] for instance, for proofs and recent references) . One of the main observation used in this contribution is the fact that an estimate of the type $0 < m(0) \le T(x,0) < M(t)$ remains valid for later time with $0 < m(t) < T < M(t)$.

- In ([15]) independent boundary conditions are assumed for $I$ and $T$ it may be more realistic to include in the description some relation on the boundary . This would make use of the boundary layer analysis briefly described in the section (8).

- A more serious difficulty comes from the opacity $\kappa_\nu(T)$ which at variant with often made hypothesis (as in [15]) is nothing but regular (cf. [14]) and very often only vaguely known. At least two options have been taken to consider this issue. In one of the first contributions on the subject (cf [16]) it was assumed that with no other hypothesis on the dependance with respect to the frequency $\nu$ the function $T \mapsto \kappa_\nu(T)$ was non increasing , while the function $T \mapsto \kappa_\nu(T)B_\nu(T)$ was non decreasing. Then some $L^1$ stability estimates lead to existence and uniqueness for the system (**??**).

  On the other hand a very "popular" (which leads to Milne problem) "grey model" is based on the assumption of independence of the opacity with respect to the frequency $\nu$. With such hypothesis several stability results has been obtained with no constraint on the regularity of the mapping $T \mapsto \kappa(T)$ (cf [2],[3],[4] ) for a first contribution in 1988 and recently (cf [10]) for the treatement of the full problem with grey opacity.

- Under some convenient scaling hypothesis, in particular large opacity with respect to the size of the media one may approximate the dynamic by a diffusion equation known as the Rosseland approximation. Once again mathematical results are well advanced for the grey model and some of its variants and more sparse in the general case. Such approximation is very well adapted to describe "interior problems" like fusion by laser confinement. It does not seem (to the best of our knowledge) present in climatology . As a matter of fact the height of the atmosphere being very small with respect to the earth radius what seems to be considered is by itself a boundary layer. . As sketched in the section 8.1 this issue is closely related to the improvement of the accuracy of the Rosseland approximation and also well developed for grey model. It is worth mentioning considering at the level of boundary layer the curvature of the atmosphere makes the problem even more subtle [25] and [24] for the Chandrasekhar equations (12).

Numerically, it is a mixed integro-differential problem for which a fixed point approach works quite well, and for which a convergence proof is available in the simpler case of Milne's.

Two methods of discretisation have been tried. A finite element method with upwinding and a semi-explicit method based on the integral form of the solution of the first equation. The second one is more precise but slower. Convergence with respect to grid refinement is fairly fast.

All should be well and yet it is not. The difficulty lies in the very large scale differences between the infrared earth radiations and the sun light. This makes the evaluation of GHG effect difficult and also because the effect is small.

The present computations validate an increase of earth temperature due to $CO_2$ and other greenhouse gases responsible for a substantial change in the transmission coefficient $\kappa_\nu$ in the lower part of the infrared frequency range emitted by earth seen as a black body at temperature 300K. However with one method the predicted increase is rather large and with another it is too small. Certainly $2^o$C increase is within the numerical predictions. But let us keep in mind that the real problem of global warming is much more complex than just radiative transfer.

# References

[1] H. Kapler and H. Hengler. Mathematics & Climate. SIAM publications. Philadelphia (2013).

[2] C. Bardos: Problèmes aux limites pour les équations aux dérivées partielles du premier ordre à coefficients réels; théor£mes d'approximation; application à l'équation de transport. (French) Ann. Sci. Ecole Norm. Sup. (4) (1970), 185-233.

[3] C. Bardos, F. Golse, and B. Perthame, The Rosseland approximation for the radiative transfer equations, Communications on Pure and Applied Mathematics, 40 (1987), pp. 691– 721.

[4] C. Bardos, F. Golse, B. Perthame, and R. Sentis, *The nonaccretive radiative transfer equations: existence of solutions and Rosseland approximation*, Journal of Functional Analysis, 77 (1988), pp. 434–460.

[5] Bensoussan, A., Lions, J.-L., Papanicolaou, G.C.: Boundary layers and homogenization of transport processes. Publ. Res. Inst. Math. Sci. 15(1), 53–157 (1979)

[6] C. Bardos, Santos, R. Sentis: Diffusion Approximation and computation of the critical size. Transactions of the American Mathematical Society Volume 284. Number 2. August 1984 pp. 617–649.

[7] K. M. Case, *Linear Transport Theory* Addison Wesley, Reading. 1967.

[8] R. Dautray and J.L. Lions, *Mathematical Analysis and Numerical Methods for Science and Technology*, Tome 3 vol 9. Chap. 21 , Springer verlag, New-York, 2000.

[9] A. Fowler, *Mathematical Geoscience*, Springer Verlag, New-York 2011.

[10] M. Ghattassi, X Huo, and N. Masmoudi *On the diffusive limit of radiative heat transfert system I: Well prepared initial and boundary condition* ArXiv:2007.13209v [math.AP] 26 Jul. 2020.

[11] F. Golse, B. Perthame, R. Sentis: The nonaccretive radiative transfer equations: existence of solutions and Rosseland approximation. J. Funct. Anal. 77 (1988), no. 2, 434–460.

[12] S. Chandrasekhar, *Radiative Transfer*, Clarendon Press, Oxford, 1950.

[13] Weinberg and Wigner *The Physical Theory if Neutrons Chain Reactors* , The University of Chicago Press, (1958).

[14] G. Pomraning *The equations of Radiation Hydrodynamics*, Pergamon Press, New-York, 1973.

[15] M. M. Porzio and O. Lopez-Pouso Application of accretive operators theory to evolutive combined conduction, convection and radiation Rev. Mat. Iberoamericana 20 (2004), 257–275.

[16] B. Mercier, application of accretive operators theory to the radiative transfer equations, SIAM J. Math. Anal. Vol. 18, No. 2, March 1987.

[17] Michael F. Modest, *Radiative Heat transfer*, $3^{rd}$ ed., Academic Press, 2013.

[18] E. Gros, Modélisation DART du transfert radiatif Terre-Atmosphère pour simuler les bilans radiatif, images de télédétection et mesures LIDAR des paysages terrestres. HAL Id: tel-00841795.

[19] C. Cornet, Transfert radiatif dans une atmosphère tridimensionnelle : modélisation et applications en télédétection. Mémoire HdR. LAb. Optique atmosphérique, Univ. Lille. 2015.

[20] James R. McCaa Mathew Rothstein Brian E. Eaton James M. Rosinski Erik Kluzek Mariana Vertenstein. User's Guide to the NCAR Community Atmosphere Model (CAM 3.0)

[21] D. Le Hardy, Y. Favennec, B. Rousseau and F. Hecht. Specular reflection treatment for the 3D radiative transfer equation solved with the discrete ordinates method. Journal of Computational Physics 334 (2017) 541–572.

[22] F. Hecht : New development in FreeFem++, J. Numer. Math., 20, pp. 251-265. (2012), (see also www.freefem.org.)

[23] G. Kanschat, E. Meinköhn, R. Rannacher, R. Wehrse (Eds) *Numerical Methods in Multidimensional Radiative Transfer*. Springer Verlag, Berlin (2000)

[24] Wu, Lei : Boundary layer of transport equation with in-flow boundary. Arch. Ration. Mech. Anal. 235 (2020), no. 3, 2085–2169.

[25] Lei Wu, Yan Guo, Geometric Correction for Diffusive Expansion of Steady Neutron Transport Equation, Commun. Math. Phys. 336, 1473–1553 (2015)

# 10 Appendix

`FreeFem++` is a convenient tool for these problems but there is a trick to compute $\int -1^1 I(\mu)\mathrm{d}\mu$ that is worth passing on.

We let the user build the mesh and initialise the constants. The domain is a rectangle $(0, Z) \times (-1, 1)$ with boundaries numbered 1 to 6 clockwise starting with $Z \times (0, -1)$; the vertical sides are divided in 2 equal parts. The following solves Milne's problem:

```
fespace Vh(th,P1);
Vh   T, I=y*(y>0), g;

func real intI(real X){ return int1d(th,5,6)(I(x+X,y));}
macro Yp() (abs(Y)+eps) // EOM
func real F(real X, real Y, real nu)
   {return  int1d(th,1)( (x<=X)*exp(kappa*(x-X)/Yp)/Yp*g(x,Y) );} // used with Y>eps
func real G(real X, real Y, real nu)
   {return  int1d(th,1)( (x>=X)*exp(-kappa*(x-X)/Yp)/Yp *g(x,Y) );} // used with Y<-eps

//////////////////////////////////////////////////////////////////////
for(int k=0;k<kmax*n; k++){ // iteration loop
    g=intI(x)*kappa/2;
    I= (y<-eps)*(  G(x,y,nu) ) + (y*exp(-kappa*x/(abs(y)+eps)) +F(x,y,nu))*(y>eps) ;
    T = sqrt(sqrt(SBsun*15*abs(g)/kappa))/pi;
    cout<< "T= " << T(0,0) << " erreur =" << int2d(th)((I-Iold)^2) << endl;
}
```